JOURNAL OF GUIDANCE, CONTROL, AND DYNAMICS
Vol. 38, No. 11, November 2015

Temporarily Captured Asteroids as a Pathway to Affordable Asteroid Retrieval Missions

Hodei Urrutxua*
Universidad Politécnica de Madrid, 28040 Madrid, Spain
Daniel J. Scheeres†
University of Colorado Boulder, Boulder, Colorado 80309-0429
and
Claudio Bombardelli,‡ Juan L. Gonzalo,* and Jesús Peláez§
Universidad Politécnica de Madrid, 28040 Madrid, Spain

DOI: 10.2514/1.G000885

The population of "temporarily captured asteroids" offers attractive candidates for asteroid retrieval missions. Once naturally captured, these asteroids have lifetimes ranging from a few months up to several years in the vicinity of the Earth. One could potentially extend the duration of such temporary capture phases by acting upon the asteroid with slow deflection techniques that conveniently modify their trajectories, allowing for an affordable access and in situ study. In this paper, a case study on asteroid 2006 RH_{120} is presented, which was temporarily captured during 2006–2007 and is the single known member of this category to date. Simulations estimate that deflecting the asteroid with 0.27 N for less than six months and a change of velocity, ΔV of barely 32 m/s would have sufficed to extend the capture for over five additional years. The study is extended to another nine virtual asteroids, showing that low-ΔV (less than 15 m/s) and low-thrust (less than 1 N) deflections initiated a few years in advance may extend their capture phase for several years, and even decades.

I. Introduction

THE growing interest in the study of asteroids, their formation, composition, or internal structure is often hindered by the lack of material samples and the difficulty of measuring certain physical features without in situ scientific experiments. Hence, the idea of capturing and bringing an asteroid into the vicinity of the Earth has gained popularity in recent years, as proven by many papers attempting to propose asteroid captures or, most recently, NASA's Asteroid Retrieval Initiative. Such Earth delivery missions would allow affordable access to asteroids along with a remarkable outcome in their scientific study, the possibility of resource utilization, and, eventually, the development of new exploration technologies for the newly coming era of manned spaceflight.

However, the affordability of such missions has been long debated due to the huge cost of applying the required ΔV to a massive object. To mitigate these difficulties, continued investigation has been devoted to the pursuit of new mission concepts and trajectory designs, as well as the selection of appropriate target asteroids, in order to reduce the mission ΔV, and hence the cost.

Reference [1] proposed exerting a small velocity change to asteroids passing close to Earth, so that zero-velocity curves close within the framework of the restricted three-body problem, hence capturing the asteroid in the vicinity of the Earth. However, their best target asteroid, 2009 BD, required as much as a 410 m/s increase of velocity. Other works, like [2], have studied not only the ΔV required to carry out the capture, but also the ΔV to transport the asteroids into the Earth's sphere of influence, combining both impulsive and low-thrust approaches. Their best candidate, 2007 CB_{27}, involved an impulsive maneuver of 700 m/s preceded by a low-thrust arc. They pointed out though that, with proper timing, a flyby with the moon could be used to provide part of the required ΔV.

References [3,4] explored the use of invariant manifolds and low-energy transfers to seek for lower ΔV capture opportunities, and they introduced the concept of easily retrievable objects, referencing a family of asteroids that could be transported into the Earth's neighborhood at a reasonably low cost. The authors provided a list of such asteroids, the best candidate being 2006 RH_{120} with a $\Delta V = 58$ m/s. Alternatively, [5] explored the possibilities of targeting asteroids that experience quasi-satellite phases, pointing out the possibility of not only extending the duration of an existing quasi-satellite state but even artificially inducing quasi-satellite phases on other asteroids, with just slight low-thrust deflections.

Most recently, NASA's Asteroid Retrieval Initiative became the first attempt of a real-life asteroid capture mission. According to the Asteroid Retrieval Feasibility Study [6], the nominally targeted asteroid, 2008 HU_4, is of approximately 500 metric tons of mass and 7–8 m diameter, and the idea is to capture it and place it in a high lunar orbit, where it would be energetically in a favorable location to support human exploration beyond cislunar space. Omitting the Earth escape trajectory, heliocentric transfer, and rendezvous with the asteroid, the sole cost of deflecting 2008 HU_4 in order to bring it into lunar orbit via a lunar flyby is estimated in a ΔV of approximately 170 m/s.

This raises the question of how much it would really take to bound an asteroid in Earth orbit and whether capturing an asteroid could be done more cheaply by targeting a different kind of asteroid or pursuing a different capture strategy. In this regard, we come to propose a novel conceptual approach to enable an affordable access to asteroids in the Earth's vicinity.

A special population of small asteroids that become temporarily captured in the Earth–moon system has recently been discovered. Although only a single member of this class of asteroids has been confirmed to date (namely, asteroid 2006 RH_{120}), rigorous calculations show that there is a significant flux of these temporary visitors

Presented as Paper 2014-0276 at the 24th AAS-AIAA Space Flight Mechanics Meetings, Santa Fe, NM, 26–30 January 2014; received 7 July 2014; revision received 24 December 2014; accepted for publication 19 January 2015; published online 26 March 2015.

*Ph.D. Candidate, Space Dynamics Group, ETSI Aeronáuticos, Pz. Cardenal Cisneros 3.
†Professor, Department of Aerospace Engineering Sciences, UCB 429. Associate Fellow AIAA.
‡Researcher, Space Dynamics Group, ETSI Aeronáuticos, Pz. Cardenal Cisneros 3.
§Professor, Space Dynamics Group, ETSI Aeronáuticos, Pz. Cardenal Cisneros 3. Lifetime Member AIAA.

[7] such that, at any given time, there are about a dozen half-meter-sized objects and at least two meter-sized objects; and one ∼10 m object would be temporarily captured every 50 years. Once captured, these near-Earth asteroids can remain bound to the Earth–moon system for times ranging from a few months up to several years. The mean lifetime of this population is predicted to be 9.5 months, during which time they make almost three orbits about the Earth. Given the small size of these asteroids, their detectability is a natural concern. According to [8], a targeted survey with enough time on a large telescope could detect the largest of these objects at a rate that might be suitable for spacecraft missions, and with enough time in advance for a rendezvous. In this regard, the authors found the existence of viable low-thrust orbital transfer paths to these objects under time-optimal constraints.

Hence, the availability of a population of temporarily captured natural satellites of the Earth–moon system, or minimoons, brings into the game new possibilities to provide humanity with access to asteroids in our own backyard. Given their expected small size, their vicinity to the Earth, and their proximity to long-term capture orbits, these bodies could enable affordable robotic and crewed missions using existing technology, as well as retrieval of substantially larger amounts of material compared to traditional sample return missions. Also, scaled versions of hazardous asteroid mitigation techniques could be tested at a fraction of the cost of current proposals. Therefore, minimoons stand out as compelling candidates for asteroid retrieval missions. The only issue would be for how long we could guarantee them to be bound in the vicinity of the Earth and, if by a convenient modification of their orbits, we could make them remain close enough to Earth for a longer time, and at what energetic cost or ΔV.

This paper contains a numerical study on what it would have taken to extend the temporary capture phase of one such minimoon (namely, the asteroid 2006 RH_{120}) during its latest 2006–2007 temporary capture. Simulations estimate that its capture could have been prolonged for five years with ΔV values as low as 32 m/s. Though the current study is founded in a past scenario, its results remain representative of the temporarily captured population of asteroids and it serves as a case study for any future minimoon of similar characteristics that we might encounter. To support this assessment, the study is also extended to nine other temporarily captured virtual asteroids, and some insight is provided on how the nature of these captures relates to the potential extension of their duration. For some of these virtual asteroids, their captures could even be extended for decades for unprecedented ΔV values of just 9 m/s.

The structure of the paper is as follows. In Sec. II, we analyze the natural capturing of asteroid 2006 RH_{120}. Next, we propose to extend the duration of its capture by first applying an impulsive ΔV (Sec. III), and then with a low-thrust deflection (Sec. IV). For the latter case, the resulting long-life orbits are studied and classified in Sec. V and, in Sec. VI, a specific search is conducted for families of certain appropriate long-life orbits, referred to as target orbits. This search procedure is then automated in Sec. VII with machine learning techniques, in order to systematically apply the same searching algorithm to the other nine temporarily captured virtual asteroids (Sec. VIII). Finally, an improvement to our asteroid capture concept is proposed in Sec. IX, and the most relevant results of the study are summarized in the Conclusions (Sec. X).

II. 2006 RH_{120} Temporary Capture

Asteroid 2006 RH_{120} is a small 5 m near-Earth asteroid discovered on 14 September 2006 during its last temporary capture, which lasted for about 472 days (370 of which were strictly spent inside the Earth sphere of influence) and extended until June 2007. As the only temporary captured object detected so far, 2006 RH_{120} is an important testbed to validate the numerical propagation model employed and study all relevant features of its complex dynamics before analyzing how to artificially influence them.

One of the goals of the study was to establish the simplest model that would reliably describe the asteroid dynamics right before, during, and after the capture. To this end, we propagated the initial conditions for 2006 RH_{120} provided by the International Astronomical Union's Minor Planet Center, and given in Table 1,¶ throughout the capture phase using models of increasing complexity. The asteroid mass has been estimated by assuming a spherical body of 5 m of diameter and a density of 2000 kg/m^3.

Table 1 Initial conditions for 2006 RH_{120} in heliocentric ecliptic J2000.0 frame (JPL 47 ephemeris)

Epoch	JD 2,454,132.5	
a	0.9873022869878605	AU
e	0.01914526201748496	—
i	0.7974471215924634	deg
Ω	278.6483110626849	deg
ω	136.132656110278	deg
M	74.85730211872003	deg

High-precision numerical ephemerides were seen to be absolutely necessary. Any attempt to use simplified ephemerides (analytical ephemerides, circularized orbits, etc.) would make the temporary capture disappear. In particular, a formulation based on the circular, or even elliptic, three-body problem would be inappropriate to model the capture dynamics, meaning that any approach based on the Jacobi (or Hill–Jacobi) constant or the Hill approximation would prove of little practical use in our case study.

Another very interesting conclusion is the fact that considering the Earth–moon barycenter (EMB) did not provide a proper reconstruction of either the trajectory or the temporary capture phenomenon. Instead, the Earth and moon should be considered as separate bodies, the position of which must be obtained from precision ephemerides, which agree with Granvik et al. [7], whose work "indicates that the presence of the Moon was of critical importance in the capture of 2006 RH_{120}." According to their statistical study, they also claimed that "not a single test particle (TP) was captured by lowering the geocentric velocity via extremely close lunar flyby's"; also, "although the Moon's orbit is the primary reason for the lack of long-lived temporarily captured objects, it is simultaneously the presence of the Moon that increases the capture probability by allowing faster objects to be captured." In Fig. 1, one can see the different trajectories that arise from considering the EMB instead of the Earth and moon as separate bodies.

As a last remark, we realized that the trajectory inside the Earth's Hill sphere is extremely sensitive to the entry conditions from the heliocentric phase. Therefore, the heliocentric propagation must be done by considering a dynamical model as realistic as possible. On the other hand, once inside the Hill sphere, a four-body model including the sun, Earth, and moon gravity is able to reproduce the temporary capture with enough reliability for our purposes. The inclusion of the J_2 gravitational harmonic would be important only for trajectories involving very close Earth approaches, which is not the case of the original 2006 RH_{120} trajectory but could be relevant for some artificially modified trajectories of the latter.

Finally, one should note that even if, according to [9], "2006 RH_{120} is small enough that solar radiation pressure is perturbing its motion perceptibly," such perturbation was not taken into account in our simulations because of the following:

1) It was verified that it has a negligible impact in the results (see Fig. 2).

2) It can be compensated during a low-thrust deflection of the asteroid, as proposed here.

In conclusion, the propagation was split in two trajectory arcs: a heliocentric arc outside the Earth's Hill sphere based on a parameterized post-Newtonian type model [10], including only gravitational source forces plus relativistic corrections; and a geocentric arc based on a four-body model including the J_2 perturbation (see

¶These values were retrieved from the JPL 47 ephemeris available online at the Jet Propulsion Laboratory, California Institute of Technology small-body database browser at http://ssd.jpl.nasa.gov/sbdb.cgi [retrieved 4 February 2014].

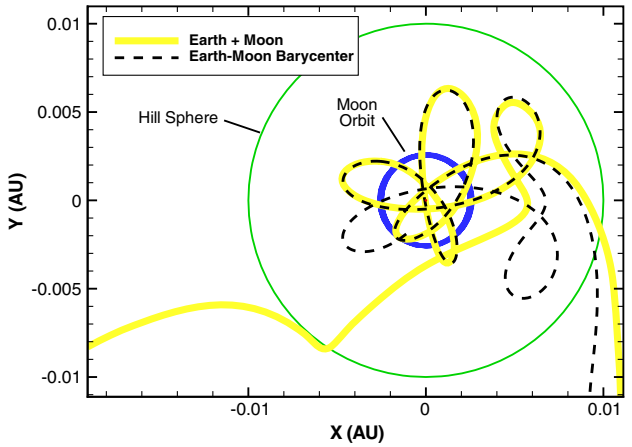

Fig. 1 Trajectories of 2006 RH_{120} using Earth–moon barycenter vs Earth and moon as separate bodies.

Table 2). The propagation is performed using a Sun-centered and Earth-centered Cowell method based on a Runge–Kutta–Fehlberg 8 (7) integrator. In Fig. 2, we compare our numerical propagations to the JPL 47 ephemeris and numerical propagations with GMAT** software as integrated from the initial conditions in Table 2.

III. Extending the Capture with an Impulsive ΔV

As defined in [7], the two requirements for an asteroid to be temporarily captured are the following:

1) Its planetocentric Keplerian energy must be negative, $E_{\text{planet}} < 0$.

2) The planetocentric distance must be less than about three Hill radii (approximately 0.03 AU). In such conditions, one could expect that a further reduction of planetocentric energy through an instantaneous negative ΔV could have the asteroid remaining in an Earth-bounded orbit for a longer period of time. As a matter of fact, if the energy reduction is large enough to raise the Jacobi constant beyond the corresponding value at L_1, the zero-velocity curves in the three-body approximation would close up at L_1 and L_2, and the asteroid would mathematically remain captured forever.

Leaving aside technological feasibility issues, one would actually not need to capture the asteroid forever but only for a long enough time, which can be obtained with a much lower ΔV. In the end, the idea is to reduce, and not to close, the gaps around the Lagrangian points to decrease the asteroid escape probability down to a sufficiently small threshold. This would provide access to the asteroid for a number of years or decades.

Extensive numerical simulation batches were run to estimate the extension of the temporary capture phase achievable for asteroid 2006 RH_{120} with a single impulsive ΔV of a given magnitude. The impulsive ΔV was seen to be most effective (in terms of extending the duration of the capture) when applied at a perigee passage and in a tangential direction. In the case of 2006 RH_{120}, the asteroid went through up to three perigee passages during its 2006–2007 temporary capture, as listed in Table 3.

The numerical analysis shows similar results, no matter which of the three perigee passages is chosen; although the results are slightly better for the third and last perigee passage, where the distance to the Earth is the minimum of all three passages. Results (propagated until no further than year 2020) are shown in Fig. 3 and reveal that a ΔV of about -36 m/s would be enough to extend the temporary capture for several extra years. This procedure provides an estimate of what it takes to artificially extend the temporary capture of an asteroid.

As a final remark, one must be cautious when considering each extended temporary capture phase, since some of the outcoming trajectories might exhibit very close Earth encounters (hence, they will be very sensitive to perturbations and uncertainties in the initial conditions) or might even be Earth/Moon impact trajectories. From the 1000 orbits simulated in Fig. 3, only one collision trajectory was detected, which was impacting with the Moon.

**GMAT (General Mission Analysis Tool) is an open-source space mission design tool developed by NASA and available at http://gmat.gsfc.nasa.gov [retrieved 2015].

IV. Extending the Capture with Low Thrust

According to the results of the previous section, a typical impulsive ΔV of over 36 m/s would be needed for a reasonable temporary capture extension. However, to provide such ΔV to a ∼130 ton asteroid might seem pretentious or technologically unrealistic. Therefore, the next logical step is to study how those estimates vary when the ΔV is not applied impulsively but instead distributed throughout a time span ΔT. For simplicity, we will consider a single thrust phase of duration ΔT and with a constant and tangential thrust magnitude F such that, after indicating with m_{ast} the asteroid mass (and neglecting the mass of the spacecraft), the following relation holds:

$$\Delta T = \frac{m_{\text{ast}} \cdot \Delta V}{F}$$

We then introduce a time delay/anticipation a_n with which the low-thrust phase begins relative to the original or unmodified third perigee passage date JD_p (see Table 3). A negative value of a_n would correspond to a thrust phase initiated before such an epoch. For convenience, we are going to measure both ΔT and a_n in days.

From a numerical implementation point of view, the asteroid orbit propagation is divided in three segments, as detailed in Fig. 4. We pick up the initial conditions of Table 1, given at epoch JD_0. Hence, the first trajectory segment is propagated, in a geocentric frame, from date JD_0 until $\text{JD}_p + a_n$. Segment 2, perturbed by a constant thrust acceleration, is then propagated forward in time for ΔT days, and then the final ballistic trajectory segment is propagated until leaving the Earth–Sun Hill sphere. Finally, the date of the Hill sphere crossing is recorded and compared to the one of the original unmodified trajectory to assess the potential benefit of the low-thrust maneuver in extending the asteroid capture duration. Unlike the impulsive case, the final results will now involve a grid search depending on three parameters (ΔV, ΔT, and a_n) and will require a much heavier simulation campaign, depending on the level of discretization employed.

A better insight into the results can be gained by looking at two-dimensional sections of the three-dimensional grid search. Most representative are the constant-ΔV sections plotted in Fig. 5, where each point represents an orbit propagation, with the given combination of a_n, ΔT, and ΔV, shaded according to how many extra days the trajectory of 2006 RH_{120} remains inside the Hill sphere. The discretization of these parameters has been enclosed to the domain $a_n \in [-330, +30]$, $\Delta T \in (0, +220]$, and $\Delta V \in [-30, -100]$; propagations are carried out until no further than year 2020, and Earth–Moon-collision trajectories have been omitted, as well as those that remain in the Hill sphere a shorter time. The grid search contained nearly 10 million points and, from all the extended duration trajectories, less than 0.02% ended up in a Moon impact, whereas the ones hitting the Earth were estimated to be less than 0.001%.

The overall look of the slices is a fractal-like structure. Although there seems to be some kind of macroscopic structure with areas of extended capture time and isles of reduced capture time, the close-ups reveal some chaoticity and scatterness of the long-life trajectories. This comes at no surprise given the highly nonlinear and time-dependent structure of our four-body problem, which is highly sensitive to initial conditions and perturbations.

From a practical point of view, it is interesting to filter our results by focusing on all trajectories providing an extended capture of, say, at least 2000 days, which is enough to enable a mission to the asteroid once captured. In addition, any trajectory leading to an Earth impact needs to be rejected. By doing so, we come to the results of Fig. 6. Notably, many filtered trajectories do not appear as isolated points.

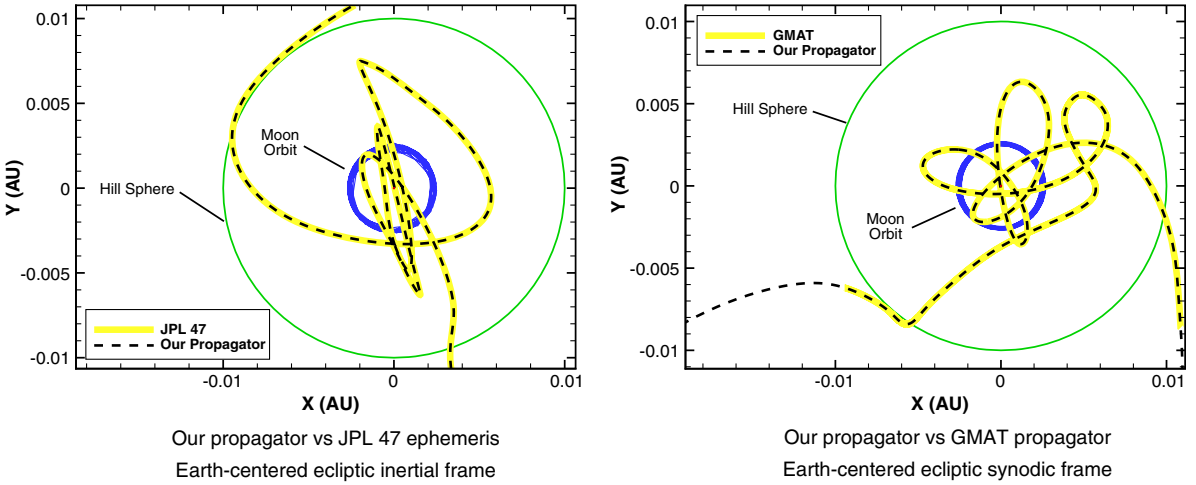

Fig. 2 Trajectory of 2006 RH_{120} during its temporary capture phase.

Instead, there appears to be some sort of continuum in the existence of long-life solutions.

We can see (Fig. 5) that a ΔV of -45 m/s is already enough to extended the capture for over 2000 extra days in the Hill sphere. However, the lowermost region of these figures (low values of ΔT) is of doubtful practical use, since it corresponds to too high values of the low-thrust intensity F. On the other side, if we raise the value of ΔV, we would increase the total impulse, but we might as well get long-life orbits within reasonable thrust values; so, it becomes a tradeoff between trying to find the lowest ΔV trajectories with the lowest thrust intensity values. We also note that a higher ΔV guarantees a higher amount of long-life orbits for many different combinations of a_n and ΔT.

V. Classifying the Resulting Long-Life Orbits

In light of the results of the preceding section, a reasonable next step is to try to understand the relation between a favorable combination of a_n, ΔT, and ΔV and the long-life orbit that it produces, as well as the key features that characterize a long-life orbit.

Some interesting observations can be made by plotting contour lines of the previously obtained long-life orbits for constant values of selected orbital elements to see how they relate to the a_n and ΔT parameters. We have done so in Fig. 6 by overlaying the values of the orbital inclinations i and the longitude of the ascending node Ω at the end of the low thrust (end of trajectory segment 2) for a ΔV of -65 m/s. This procedure highlights some interesting features of the orbit of 2006 RH_{120}. For example, at the end of the low-thrust phase, all orbits end up having $i \in (88\ \text{deg}, 110\ \text{deg})$ and $\Omega \in (100\ \text{deg}, 130\ \text{deg})$, i.e., they are retrograde with respect to an ecliptic frame. This was expectable, since these orbits are variations

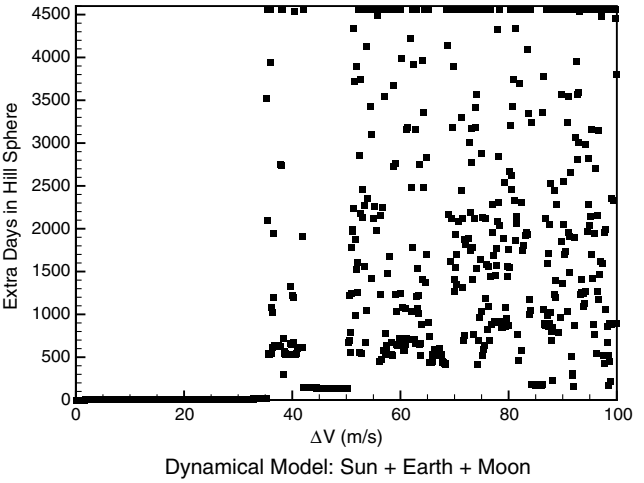

Fig. 3 Extension of 2006 RH_{120} capture with impulsive tangential ΔV.

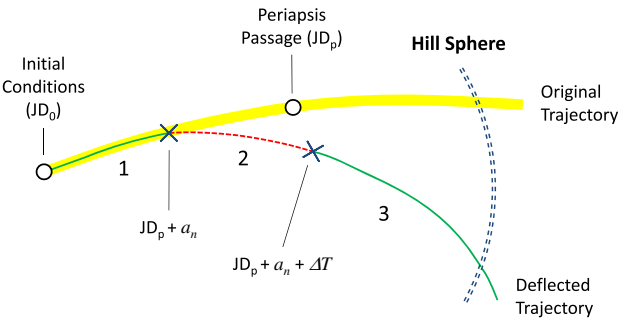

Fig. 4 Numerical integration procedure, splitting the orbit propagation in three segments.

Table 2 Perturbations considered in our numerical propagations

Outside Hill sphere	Inside Hill sphere
All eight planets + Pluto	Sun + Earth + moon
Ceres, Pallas, and Vesta	Earth J_2
Apparent Sun J_2	Thrust (if applied)
Relativistic corrections	
Thrust (if applied)	

Table 3 Julian dates of perigee passages of 2006 RH_{120} during its 2006–2007 temporary capture

Perigee passage	Julian date	Calendar date
1	2,454,104.251673	2007 January 03
2	2,454,184.021830	2007 March 25
3	2,454,265.729196	2007 June 14

of the unmodified orbit, which was retrograde too. Similar observations can be done for the rest of orbital elements and different values of ΔV. Note that orbital elements may not be the most appropriate way to describe the motion in this multibody regime. The use of a more pertinent parameterization could shed more light on the problem; although, in practice, the orbital elements proved both convenient and useful for the current study.

A probably more convenient way to visualize it is by using scatter plots, where each point represents an orbit propagation with a given combination of parameters a_n, ΔT, and ΔV; and the axes may be any of the orbital elements. This approach provides not only the values of the orbital elements of the long-life orbits but also how they relate to each other. In addition, it allows filtering the trajectories according to

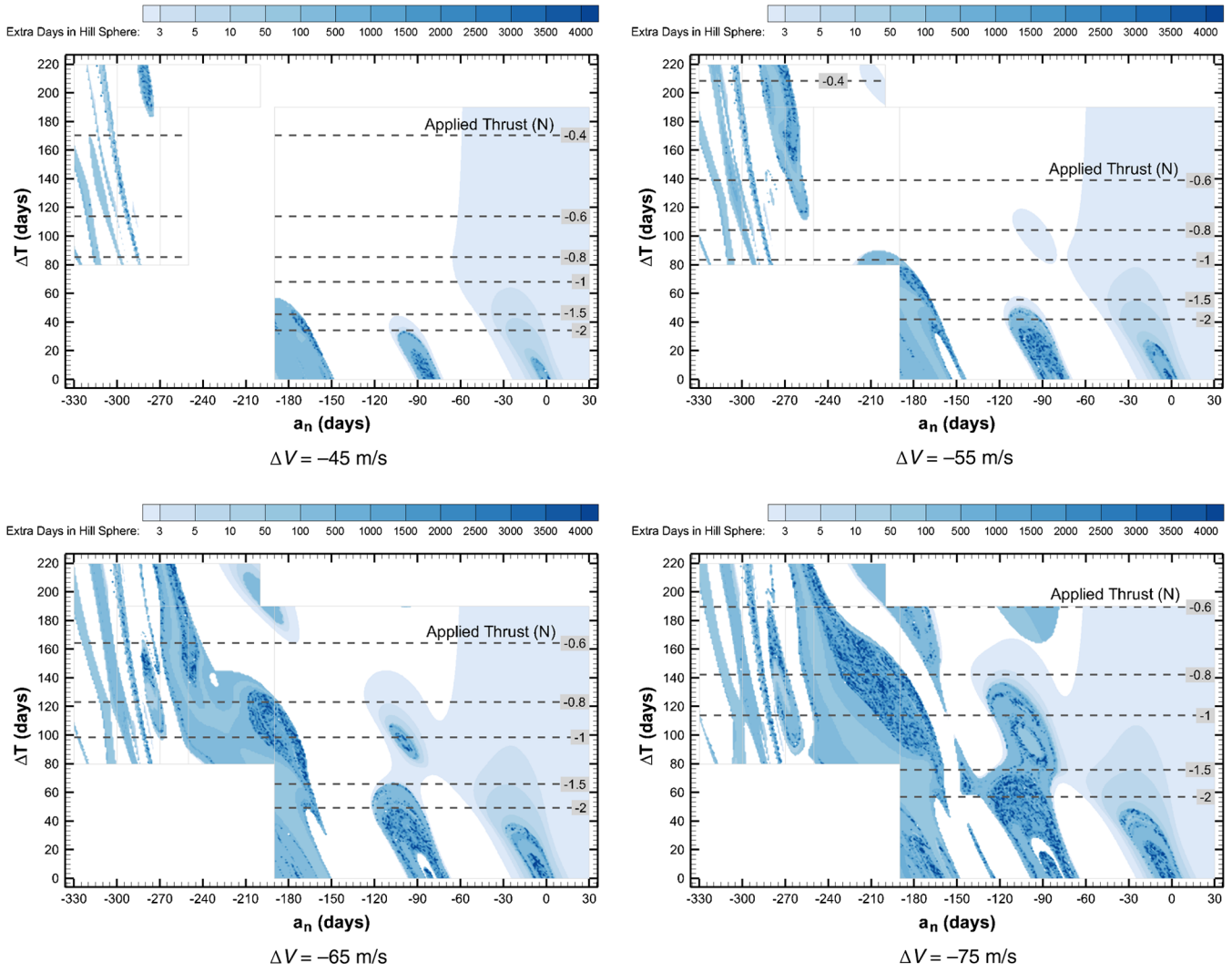

Fig. 5 Two-dimensional grid searches in parameters a_n and ΔT for different fixed values of ΔV.

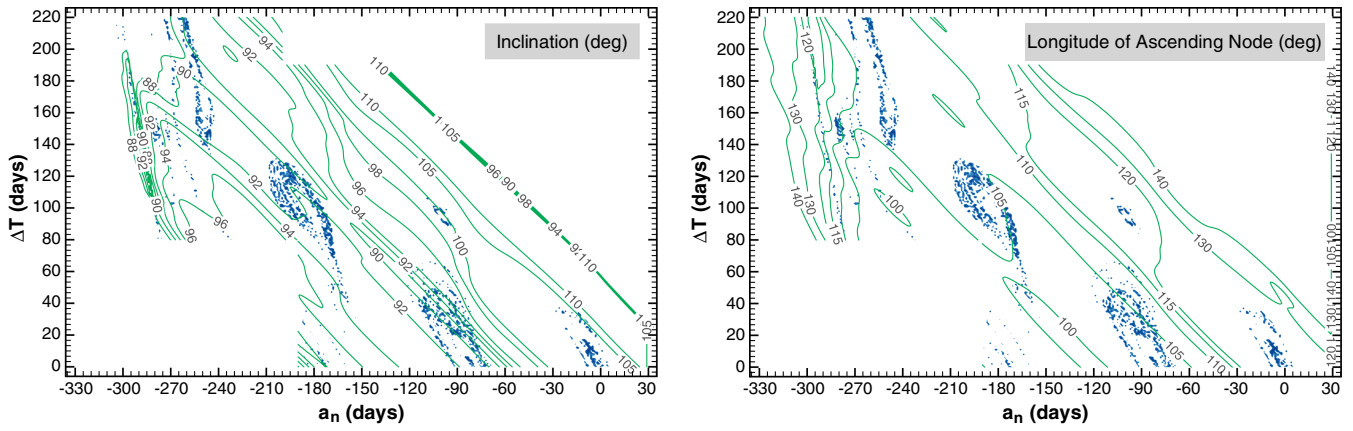

Fig. 6 Long-life trajectories for $\Delta V = -65$ m/s with contour lines for orbital element values.

other criteria; for example, minimum permanence inside the Hill sphere, maximum low-thrust magnitude, and so on. For instance, in Fig. 7, the relations $i(a)$ and $i(e)$ are shown for values of ΔV ranging from -40 to -80 m/s, where each point represents an orbital propagation, shaded according to how many extra days the resulting trajectories remain inside the Hill sphere and excluding trajectories lasting less than 2000 extra days or requiring a thrust over 1 N, which could be realistic mission constraints. Interesting conclusions can be drawn by the thorough observation of such plots, although the amount of resulting graphics is quite overwhelming, since one cannot only see how elements relate to each other but also how they relate to the parameters a_n, ΔT, or ΔV (see Fig. 8).

Statistical information can be obtained by the use of histograms instead of scatter plots. It allows a quick overall view of the types of orbits that arise for the given value (or range of values) of ΔV, independently of the values or parameters a_n and ΔT. The histograms with statistical counts confirm more straightforwardly some of the conclusions we could draw from Figs. 6 and 7 on the range of the

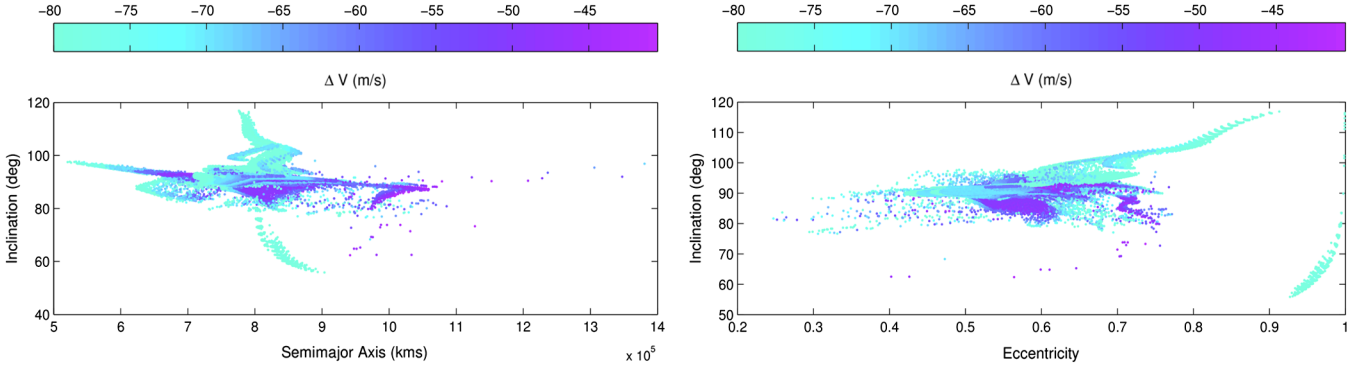

Fig. 7 Relation between orbital elements for long-life trajectories with $\Delta V \in [-80, -40]$ m/s.

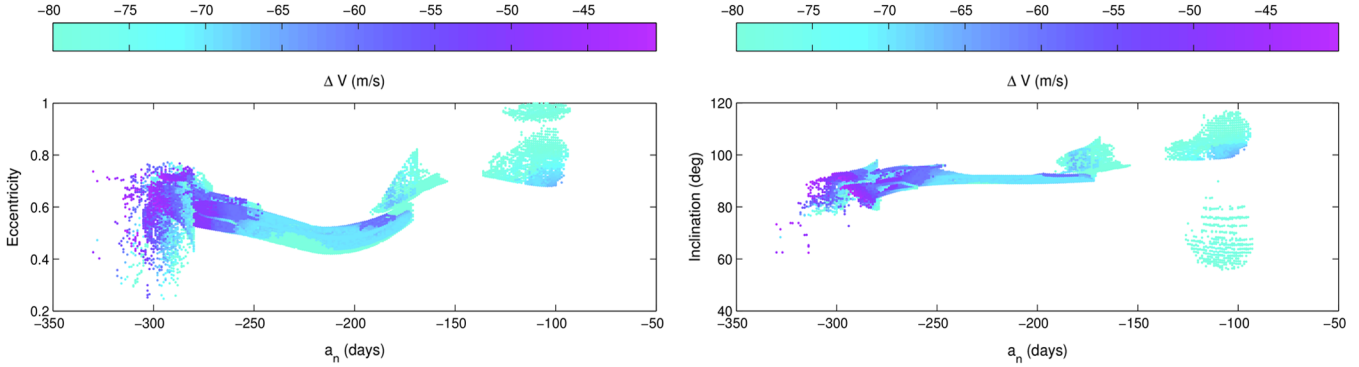

Fig. 8 Eccentricity and inclination as a function of a_n for long-life trajectories in $\Delta V \in [-80, -40]$ m/s.

values of orbital elements of the orbits, and they confirm aspects such as most of the orbits being retrograde or most orbits ending up with semimajor axes on the order of twice the lunar distance.

VI. Seeking Long-Life Target Orbit Families

The results of the previous sections suggest that reaching a certain target orbit at the end of the low-thrust phase might be a sufficient condition to guarantee a long lifetime before escaping the vicinity of the Earth. The next step is to try to group these target orbits into orbit families based on the control parameters a_n, ΔT, and ΔV, and their orbital elements.

Figure 9 is a scatter plot with axes a_n and ΔT, containing all trajectories of the grid search lasting over 4000 days and requiring less than 1 N thrust. The trajectories are shaded, both according to the ΔV and the thrust required. One can visually detect areas or zones in the map that correspond to adequate tradeoffs between a low ΔV and a low thrust. Eight promising zones have been identified and catalogued as zones A to H, conveniently illustrated in Fig. 9 and described in Table 4.

To check whether the trajectories lying in zones A to H yield similar orbits at the end of the low-thrust segment, we used the same approach as in Fig. 7, i.e., plotting combinations of their orbital elements but filtering the data such that only trajectories inside these zones are shown. Figure 10 shows the relation between different

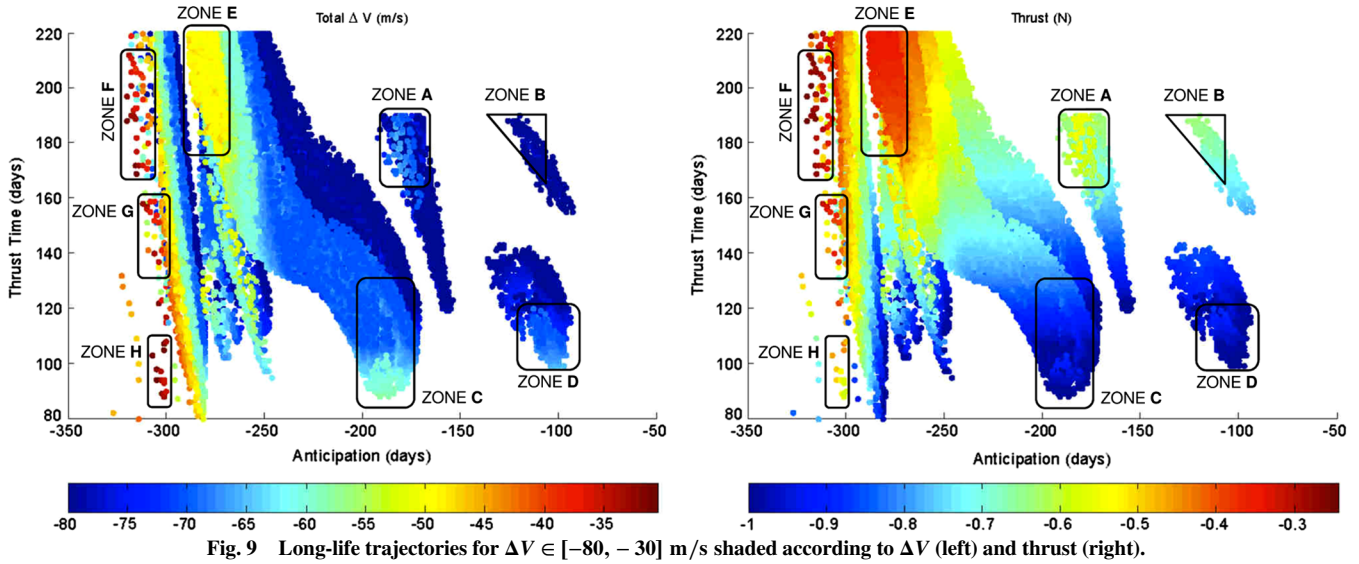

Fig. 9 Long-life trajectories for $\Delta V \in [-80, -30]$ m/s shaded according to ΔV (left) and thrust (right).

Table 4 Approximate bounds of zones A to H in the domain of parameters a_n and ΔT

Zone	$a_{n,\min}$	$a_{n,\max}$	$\Delta T_{\min}$	$\Delta T_{\max}$
A	−190	−170	160	190
B	−140	−90	150	190
C	−190	−170	80	140
D	−115	−95	95	120
E	−290	−265	170	220
F	−320	−310	165	215
G	−315	−295	135	160
H	−313	−295	85	110

orbital elements for zones A to E, highlighting an important fact: these final orbits, which we could refer to as *"target orbits,"* appear to be mostly grouped together in families with similar orbital elements. Therefore, these zones are in fact families of target orbits that seem to guarantee an extended permanence inside the Hill sphere at a given balance between low ΔV and low thrust.

The A and B families of target orbits offer interesting tradeoffs between thrust and ΔV values, where the latter shows a more compact structure but at a higher ΔV. The C family (and to some extent, the D family) does not contain well-balanced tradeoffs but does exchange higher thrust values (close to 1 N) for the benefit of a lower ΔV. The E family offers an appealing combination of ΔV below 50 m/s and thrust values below 0.5 N; it covers a wide range in the domain of parameters, and it is extremely compact, highly dense, and safe in the sense that any neighboring orbit is a long-lifetime orbit. Families F to H show a rather sparse or scattered structure in Fig. 9, but with considerably lower ΔV values. From the whole grid search, family F is notoriously the best-balanced family, offering both the lowest ΔV (below 40 m/s) along with the lowest thrust levels (below 0.3 N).

Next, with the purpose of selecting the most attractive target orbits within each family, a few samples of target orbits with low ΔV and thrust values have been extracted from families A, C, E, and F. The samples are reported in Tables 5–8, respectively, providing the corresponding thrust parameters (a_n, ΔT, and ΔV) that lead to those orbits. Among the most favorable orbits, the best results come from orbits within the families E and F. For the E family, we notice an impressive combination of a ΔV as low as 47.5 m/s along with a thrust of around 0.33 N. The best F family orbit shows a ΔV of less than 31 m/s and a thrust below 0.28 N, with a deflection beginning 315.5 days before the original third perigee passage (see Table 3) and lasting for about 172 days.

Extending the grid search even further, or using a finer grid size in the domain of the thrust parameters, it is reasonable to assume that even slightly better target orbits might be found. However, we believe the current results are already representative enough, both qualitatively and quantitatively, of the cost of extending the temporary capture of 2006 RH_{120}.

As for the chaoticity of the selected best candidate orbits, additional numerical simulations were performed by using a denser grid search. It was observed that these target orbits are robust in the sense that, even if errors are introduced in the initial conditions or thrust parameters, if they are small enough, the resulting orbits still ensure the required capture duration. The time evolution of different neighboring target orbits, like those in Tables 5–8, has also been analyzed. It was seen that, even if all the orbits initially begin with closely similar values of the thrust parameters, they slowly diverge as time goes by (see Fig. 11), as expected from the four-body dynamics of the problem. However, the eventually large variations in the final conditions of each orbit are not of concern as long as the permanence time in the Hill sphere can still be guaranteed. These variations in the final orbital state manifest the orbital elements do not provide the most appropriate description of the problem, although locally and for short time spans, where variations are small, they do serve the purpose.

Finally, a numerical check has been conducted to verify the suitability of the proposed fully tangential deflection maneuver. It is well known that tangential thrust maximizes the instantaneous rate of energy increase for the two-body problem with constant thrust. In addition, a fully tangential strategy can also be proven to be the asymptotic solution for maximizing the orbital energy increase during a fixed period of time in the low-thrust case [11]. Nevertheless, the doubt remains whether a noteworthy improvement can be obtained in our more complex scenario by allowing the thrust direction to change with time. To this end, the optimal control problem of finding the thrust orientation law that minimizes the constant thrust F needed to cover the thrusted arc of a given target orbit has been formulated. Note that, since ΔT is fixed, this corresponds to minimizing ΔV. The only constraints are the state of the orbit at the extremes of the arc, given by their values in the original, tangential thrust solution. A direct transcription method has been implemented numerically, providing the optimal thrust control angle. Simulations for selected C family target orbits show the optimal time evolution of the thrust control angle remains relatively small (variations of β are on the order of 10^{-2} deg) and the corresponding control law yields a negligible improvement. This points out that the target orbits obtained in the grid search are already quasi optimal and, given the great increase in computational cost of this kind of optimization, its use is not justified for this study.

VII. Automation of the Search for Target Orbits

The search procedure described in the previous section is mostly manual and involves thorough observation of the data, a decision-making process, and several iterations until arriving at the final target orbits. This is a time-consuming process, especially when several candidate asteroids need to be analyzed. For this reason, a much more efficient strategy based on machine learning techniques has been implemented and is described in this section.

A first step in the implementation of the algorithm is to establish a feature vector $\boldsymbol{x}$ containing the variables that form the parametric domain of where to identify or classify alike orbits into families. A convenient feature vector can be constructed from the orbital elements at the end of the thrust arc together with the corresponding epoch (JD), i.e.,

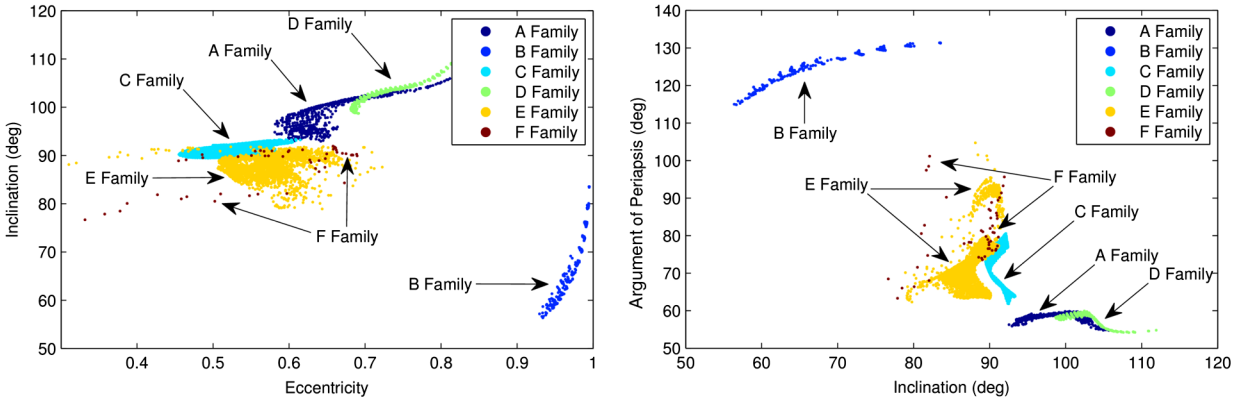

Fig. 10 Relation between different orbital elements for target orbit families A to E.

Table 5 Sample of target orbits with low values of ΔV and thrust, extracted from the A family

a, days	ΔT, days	ΔV, m/s	Thrust, N	Extra, days	a, km	e	i, deg	Ω, deg	ω, deg	ν, deg
−183.0	188.5	−66.6	−0.5353	4,555	866,688	0.657	100.65	111.98	59.27	142.39
−183.0	188.8	−66.6	−0.5344	2,442	867,494	0.659	100.72	112.01	59.21	143.02
−182.7	189.0	−66.7	−0.5347	4,555	868,237	0.664	100.86	112.10	59.08	144.17
−183.4	189.2	−66.7	−0.5341	4,555	867,533	0.658	100.67	111.96	59.22	142.99
−182.4	188.5	−66.8	−0.5369	4,555	867,431	0.664	100.85	112.11	59.12	143.86
−183.3	189.4	−66.8	−0.5343	4,555	867,965	0.661	100.75	112.00	59.15	143.68

Table 6 Sample of target orbits with low values of ΔV, extracted from the C family

a, days	ΔT, days	ΔV, m/s	Thrust, N	Extra, days	a, km	e	i, deg	Ω, deg	ω, deg	ν, deg
−188.0	88.6	−58.0	−0.9918	2,892	837,240	0.557	92.29	107.31	77.86	254.83
−187.5	88.6	−58.0	−0.9918	2,090	838,403	0.560	92.29	107.27	77.71	257.06
−187.5	88.8	−58.0	−0.9896	4,555	839,013	0.560	92.29	107.27	77.68	258.08
−187.0	88.8	−58.0	−0.9896	4,555	839,973	0.562	92.29	107.21	77.53	260.48
−189.0	89.0	−58.0	−0.9873	4,555	836,083	0.553	92.29	107.40	78.09	252.46
−187.5	89.0	−58.0	−0.9873	4,555	839,595	0.560	92.28	107.26	77.64	259.13

Table 7 Sample of target orbits with low values of ΔV and thrust, extracted from the E family

a, days	ΔT, days	ΔV, m/s	Thrust, N	Extra, days	a, km	e	i, deg	Ω, deg	ω, deg	ν, deg
−286.0	215.0	−47.5	−0.3347	4,555	817,634	0.596	85.02	110.80	71.11	157.38
−276.0	215.0	−47.5	−0.3347	4,512	787,183	0.528	87.30	107.69	67.10	173.01
−287.0	218.0	−47.5	−0.3301	4,555	815,161	0.593	84.05	110.13	70.11	161.76
−276.0	218.0	−47.5	−0.3301	4,555	788,109	0.523	88.05	108.92	65.27	179.42
−283.0	220.0	−47.5	−0.3271	4,555	802,661	0.551	84.79	108.27	67.68	171.94
−280.0	220.0	−47.5	−0.3271	4,555	795,747	0.531	86.35	108.59	65.88	177.23

Table 8 Sample of target orbits with low values of ΔV and thrust, extracted from the F family

a, days	ΔT, days	ΔV, m/s	Thrust, N	Extra, days	a, km	e	i, deg	Ω, deg	ω, deg	ν, deg
−315.4	172.4	−31.4	−0.2759	4,555	720,321	0.661	91.66	122.09	92.25	184.16
−315.5	172.8	−31.3	−0.2744	4,555	721,254	0.656	91.68	122.13	92.28	184.76
−315.5	172.9	−31.3	−0.2743	4,555	721,567	0.655	91.68	122.15	92.28	184.97
−315.5	172.2	−31.2	−0.2745	4,555	719,058	0.661	91.70	121.94	92.52	183.64
−315.5	172.3	−31.2	−0.2743	4,555	719,354	0.659	91.70	121.96	92.52	183.84
−315.5	172.4	−31.2	−0.2742	4,555	719,660	0.658	91.70	121.97	92.52	184.04

$$\boldsymbol{x} = \{a, e, i, \Omega, \omega, \nu, \mathrm{JD}\}$$

Next, a set of variables containing information relevant to the family classification criteria needs to be grouped into an output vector $\boldsymbol{y}$, which is here conveniently defined as

$$\boldsymbol{y} = \{F, \Delta V, a_n, \Delta T\}$$

Hence, the functional application $\mathcal{G}$: $\mathbb{R}^7 \rightarrow \mathbb{R}^4$ relating the two previously defined vectors

$$\boldsymbol{y} = \mathcal{G}(\boldsymbol{x})$$

corresponds to orbit propagations starting from a set of given initial conditions for a given asteroid, such that, for given thrust parameters $\{a_n, \Delta T, \Delta V\}$, the deflected trajectory has orbital elements $\{a, e, i, \Omega, \omega, \nu\}$ by the end of the thrust arc at epoch JD. To search for target orbits, the application $\mathcal{G}$ should be restrained to only those deflected trajectories yielding a minimum permanence in the Hill sphere, which are a subset of all the trajectories precomputed in a grid search.

The main inconvenience in working with the aforementioned scheme is that the feature vector $\boldsymbol{x}$ is too high-dimensional to deal with it manually or try to visualize it graphically. Fortunately, this difficulty can be alleviated by resorting to principal component analysis (PCA) [12]. PCA is a mathematical procedure based on using an orthogonal transformation to convert a set of data of possibly correlated variables $\boldsymbol{x}$ into a set of values of linearly uncorrelated

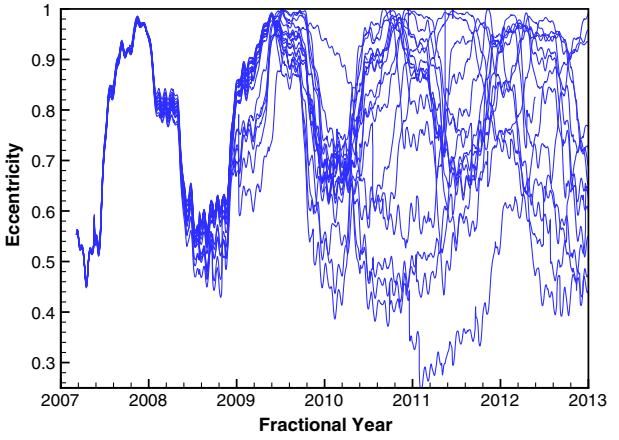

Fig. 11 Time evolution of eccentricity for 19 random C family target orbits.

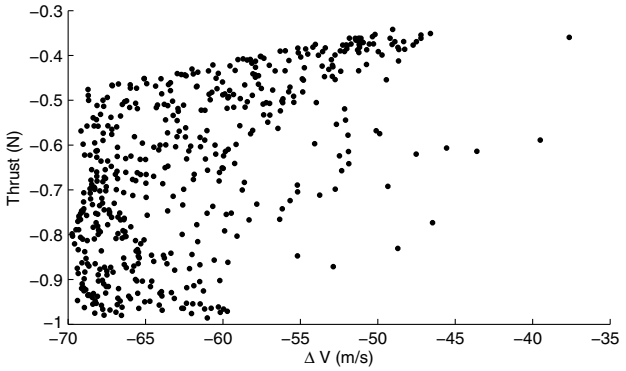

Fig. 12 Relation between ΔV and F for centroids of clusters after applying K-means algorithm.

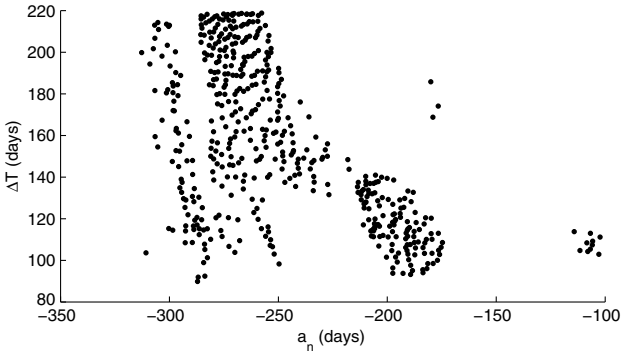

Fig. 13 Centroids of clusters expressed in the domain of parameters a_n and ΔT.

variables z called principal components, which allows us to reduce the dimension of the feature vector. The transformation is defined in such a way that the first principal component has the largest possible variance, and each succeeding component, in turn, has the highest variance possible under the constraint that it be orthogonal to (i.e., uncorrelated with) the preceding components.

If we filter the grid search data so that we only consider trajectories with $|\Delta V| \leqslant 70$ m/s, $|F| \leqslant 1$ N, and over 2000 extra days in the Hill sphere, we can work with a reduced-dimension feature vector z of dimension five (i.e., $k = 5$) while still preserving 94.4% of the variance. This provides a convenient dimensionality reduction in the domain of features at the cost of a negligible loss of information.

Now that the features of the target orbits have been reduced to just five, the classification of the orbits into groups can be performed. For that purpose, we employ a clustering machine learning technique known as the K-means algorithm [13]. This algorithm aims to partition m data points into K clusters in which each data point belongs to the cluster with the nearest mean. The main idea behind the proposed algorithm is to try to identify the existence of a predetermined number of K clusters represented by their centroids by assigning each point in the dataset to the centroid with the nearest mean. At each iteration, the centroids are relocated and the data points reassigned again to the new centroids. After iteratively repeating this process, the positions of the centroids converge and the K clusters become defined by the group of points belonging to each of the K centroids.

The K-means algorithm has been applied by setting $K = 500$, hence reducing the candidate target orbits into 500 clusters represented by their centroids of coordinates $z_k = \{z_1, z_2, z_3, z_4, z_5\}$ in the domain of reduced features, and containing homogeneous groups of target orbits that share alike features. For each cluster, the required ΔV and thrust magnitude F to guarantee a given capture extension can be analyzed. Figure 12 shows these results for asteroid 2006 RH_{120} and assuming a required capture extension of at least 2000 days; such a graph is useful to select the cluster containing the target orbits with the desired compromise between ΔV and thrust.

Finally, in order to try to reproduce the same results of the previous section, it is enough to request our machine learning algorithm to select the lowest ΔV cluster. Doing so, and looking at the orbital elements of the selected cluster, we find that the results of our machine learning technique coincide with those obtained manually. As shown in Fig. 13, the selected clusters mostly match families A to H of the $\Delta T(a_n)$ diagram of Fig. 9, with the advantages that the machine learning process is fully automated (taking the human component and decision making out of the process); provides the solution within minutes (as compared to the manual procedure that may take several hours); and can straightforwardly be applied to any other asteroid, provided a grid search has been computed.

However, two main differences must be pointed out:

1) Centroids tend to populate the most dense areas; thus, the cluster density depends on the grid search discretization as well as the filtering thresholds, so the cluster density is also an indicator of the robustness of the orbits within the clusters. That explains why families A and D barely contain a handful of clusters and the B family does not contain a single cluster, whereas families C and E are very heavily populated.

2) As cluster values are the mean values of the orbits within the cluster, for isolated clusters (hence less robust), the cluster value may be slightly overestimating the lowest ΔV orbits, since orbits belonging to isolated clusters may have a large variance.

These issues are common and depend on the sample orbits, the total number of clusters K, and the fine tuning of the K-means algorithm; and they can be accounted for if a more precise solution was needed, which is beyond our current purpose.

VIII. Reproducing the Results for Different Asteroids

The proposal of prolonging the temporary capture phase of an already captured asteroid has proven very successful and far more efficient, in terms of the required ΔV, than previous asteroid retrieval proposals [1–6] (see Table 9). Although 2006 RH_{120} is the only known asteroid of this kind, new ones are expected to be discovered [7,8]. This means that the procedure described in the previous section could indeed be applied each time a new temporarily captured asteroid is observed, as long as the detection is conducted early enough so that a deflection mission could be planned.

Reference [7] contains a statistical study of the population of temporarily captured objects, made with Monte Carlo methods after creating a virtual population of fictitious asteroids or test particles and statistically studying their features; their following orbits; and, eventually, their temporary captures. The idea here is to apply the capture extension technique described in the previous sections to selected test particles, compute the low-thrust ΔV requirements, and compare them to the ones obtained for asteroid 2006 RH_{120}.

Initial conditions for several such test particles were kindly provided by the authors of the previous reference [7] so that a similar deflection procedure as for 2006 RH_{120} could be applied to nine arbitrary fictitious asteroids. All nine test particles do have a temporary capture phase, since their planetocentric energy becomes negative at the same time they are within a three-Hill-radius distance from the Earth. Their trajectories (in synodic geocentric ecliptic frame coordinates) and Earth-binding energies (EBEs) are shown in Fig. 14; and the duration of their temporary capture phases, as well as the number of times they revolved around the Earth (in a synodic

Table 9 Comparison with existing literature

Authors	References	Asteroid	Lowest ΔV, m/s
Hasnain et al. (2012)	[2]	2007 CB_{27}	>700
Baoyin et al. (2010)	[1]	2009 BD	400
Brophy et al. (2012)	[6]	2008 HU_4	170
Yárnoz et al. (2013)	[4]	2006 RH_{120}	58
Current paper	— —	2006 RH_{120}	31.2

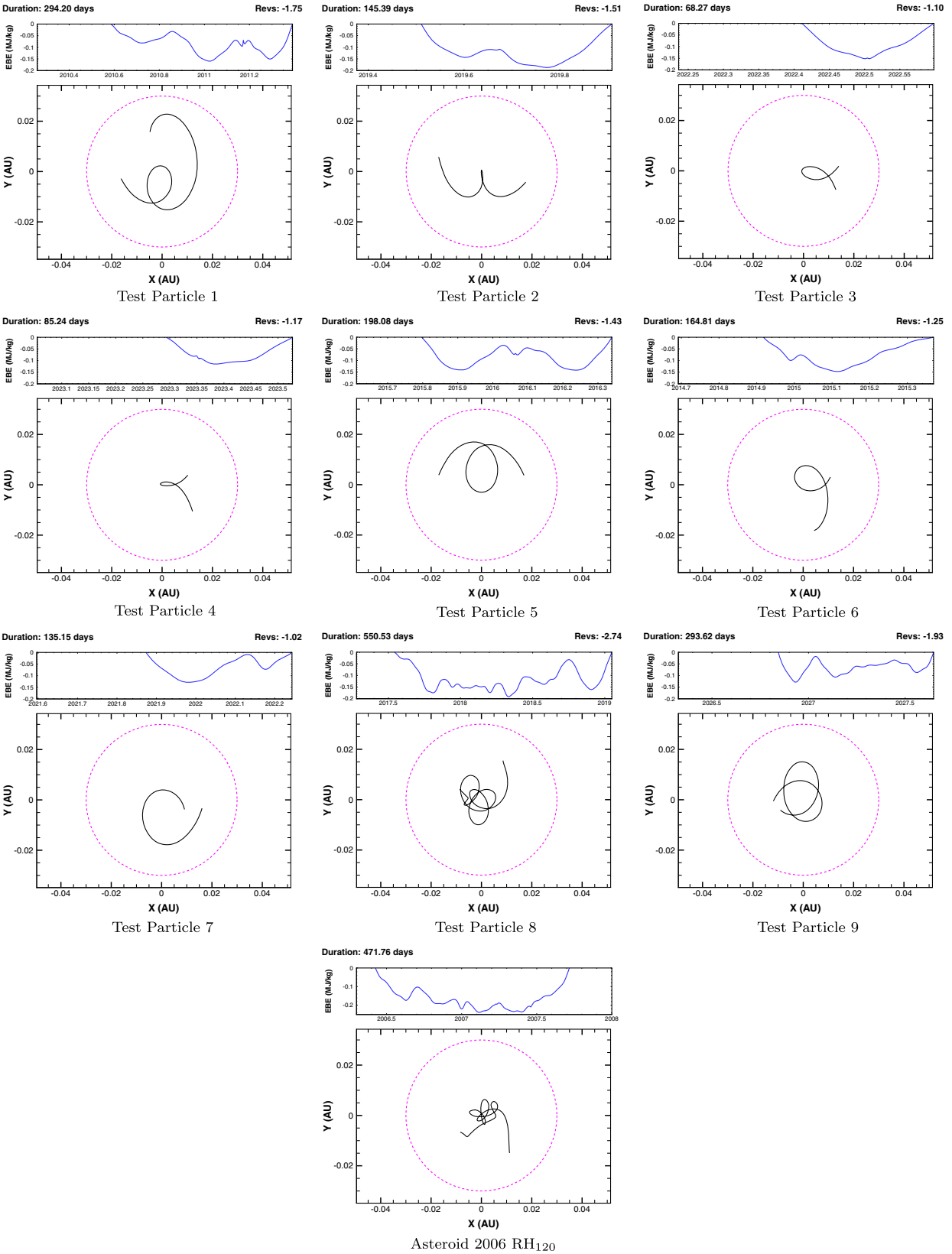

Fig. 14 Trajectories of the nine test particles and 2006 RH_{120} during their temporary capture phases.

frame), are shown in Table 10. The three-Hill-radius distance is also displayed as a dashed circle.

A first glance at the temporary capture phases of these test particles reveals some typological differences with respect to asteroid 2006 RH_{120}. Whereas 2006 RH_{120} revolves several times around the Earth during a temporary capture that lasts for 472 days in total (and a great part of its trajectory, 370 days, happens inside the Hill sphere), these test particles, with the only exception of test particle (TP 8), have shorter temporary captures (some even much shorter, such as TP 3 and TP 4), complete fewer revolutions around the Earth (except TP 8), and their trajectories happen mostly outside the Hill sphere, except for occasional close encounters at perigee passage; so, it might seem

Table 10 Description of temporary capture phases of nine test particles provided by the authors of [7][a]

Test particle identification	Days from beginning of temporary capture to perigee passage	Duration of temporary capture, days	Number of revolutions around Earth	Approximate impulsive ΔV to extend temporary capture over 1000 extra days, m/s
TP 1	218.34	294.20	−1.75	−80
TP 2	59.59	145.39	−1.51	−15
TP 3	33.85	68.27	−1.10	−70
TP 4	22.52	85.24	−1.17	−60
TP 5	101.01	198.08	−1.43	−85
TP 6	28.47	164.81	−1.25	−100
TP 7	111.98	135.15	−1.02	−25
TP 8	130.97	550.53	−2.74	−65
TP 9	69.83	293.62	−1.93	Cannot extend up to 1000 days

[a]Negative revolutions mean the orbit around the Earth is retrograde in a synodic frame.

like 2006 RH_{120} is somewhat better behaved than most of these nine test particles. Note that all of these test particles complete retrograde relative orbits around the Earth; according to [7], this is statistically true for two-thirds of the population of temporarily captured objects.

As a first step, we evaluate the required impulsive ΔV to be applied at perigee passage to extend the temporary capture phases over 1000 extra days. Results are included in the last column of Table 10, ranging from values as low as −15 m/s for TP 2 up to −100 m/s for TP 6, which are coherent with the −36 m/s we calculated for asteroid 2006 RH_{120}. Note that, for TP 9, we could not extend the temporary capture beyond a few hundred extra days, at least for reasonable values of ΔV.

Placing the values of Table 10 in scatter plots, as in Fig. 15, allows us to look for possible relationships between the duration of the temporary capture, the number of revolutions completed around the Earth in a synodic frame, and the impulsive ΔV at perigee required to extend the temporary capture over 1000 extra days (for each of the nine test particles), as well as see whether these values are somehow correlated. It turns out that, although the duration of the capture and the number of revolutions are correlated approximately linearly (not shown in Fig. 15), these two variables do not correlate in any clear manner with the impulsive ΔV.

The next step in our procedure is to perform a grid search in the parameters a_n, ΔT, and ΔV for each of the test particles. For asteroid 2006 RH_{120}, we chose to constrain the domain of a_n to values such that we would explore only trajectories where the low-thrust deflection started once inside the Hill sphere, but not before. For some of these test particles, however, this happens to be a very short time span, since the capture begins shortly before the perigee passage. Consequently, the whole ΔV would need to be applied in a short time, which might lead to high values of the thrust intensity. In the same manner, for 2006 RH_{120}, we estimated the prolongation of its temporary capture by measuring the extra days or permanence inside the Hill sphere. For this set of test particles, however, we preferred to refine our estimates and measure instead the true prolongation of the temporary capture phases (which, in most cases, end outside the Hill sphere) by stopping the integration when the planetocentric energy becomes positive or the three-Hill-radius sphere is exited.

Right after computing the grid searches, we proceed to apply the machine learning algorithm explained in the previous section to each of the test particles. To compute the thrust intensity, we assumed the test particles were of the same size and mass as 2006 RH_{120}; although according to [7], the temporary captured asteroids are statistically smaller than 2006 RH_{120}, so thrust intensities should be accordingly lower.[††] Table 11 gathers the results of the grid searches, where our machine learning algorithm has picked up the mean values of the clusters with the lowest thrust intensity value among orbits lasting over two extra years, or five extra years temporarily captured. Hence, values in Table 11, as compared to those of Table 10, show the cost of extending the duration of the temporary capture when using a low-thrust deflection instead of an impulsive burn at perigee passage.

As we can see from this subset of temporarily captured asteroids, as a general rule, the low-thrust deflection requires a higher ΔV, apparently showing a higher increase of ΔV when the temporary capture begins right before the perigee passage (i.e., only a few days earlier), as for TP 2, TP 3, or TP 4. However, examples of the opposite behavior are also found, as for TP 6. It is significant that those test particles demanding a considerably higher ΔV than for an impulsive maneuver (namely, TP 2, TP 3, and TP 4) also have closer approaches to the Earth and that their trajectories seem more strongly perturbed, whereas test particles decreasing the amount of necessary ΔV, such as TP 6 and TP 7, have smoother relative trajectories around the Earth and higher perigees.

Additionally, one can see that, for most test particles, it does not make a great difference to prolong the temporary capture for two additional years, or five years, as if longer temporary captures were obtained at a smaller marginal cost or additional ΔV. Thus, extending the capture from two to five extra years implies only a slight increase of the ΔV and thrust intensity for most asteroids of our population sample. Again, there are exceptions, like TP 1, for which the thrust intensity nearly doubles or, like TP 5, for which not only the required thrust is nearly twice as much but the ΔV is also much higher.

Overall, attending at the energetic cost of extending the temporary capture of these nine asteroids, and presumably of any other average temporarily captured asteroid, the ΔV needed with a low-deflection technique is less than the other asteroid retrieval missions proposed in the literature. Thus, asteroid 2006 RH_{120}, which we have studied in detail throughout the present paper, does look like a representative member of the population of temporarily captured asteroids, in terms of ΔV requirements. However, the required thrust for these test particles is, in many cases, beyond reasonable for practical applications. Except for TP 7 and TP 8, for which the temporary captures could be greatly extended with only −0.8 and −1.18 N, respectively, the other test particles would require a thrust level quite beyond 1 N. Nevertheless, we remind the reader that these thrust estimations are based on a 5-m-diam asteroid, and if the asteroid were smaller, the thrust requirement would drop considerably; for instance, a 2-m-diam asteroid would reduce the required thrust intensity by a factor 15.6 and, similarly, for a 1-m-sized asteroid, the thrust would be 125 times smaller.

IX. Deflecting Asteroids Before the Beginning of Temporary Capture

Given the somewhat large thrust magnitude requirements for prolonging the temporary capture of the asteroid test cases described in the previous section, alternative deflecting strategies should be considered. In particular, it was seen that, when the natural capture phase is relatively short, as is the case for many of the test particles here considered, the consequent thrust magnitude requirements rapidly grow simply due to the constraint of having to apply the thrust during the capture phase. Therefore, it seems logical to attempt to deflect the asteroids earlier, i.e., before their temporary captures

[††]For instance, if these test particles were half the size (in diameter) of 2006 RH_{120}, the required thrust levels would be eight times smaller than those shown in Table 11.

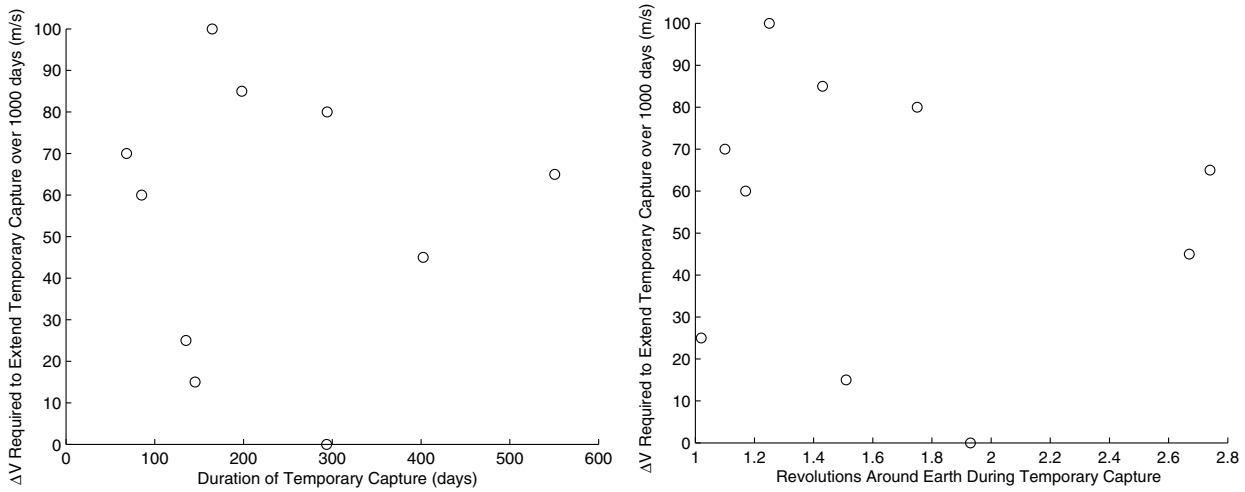

Fig. 15 Properties of the capture of the nine test particles.

begin. The purpose is double: on the one side, it can be expected that appropriately modifying their entry trajectories could result in better behaved and longer-lasting capture phases. On the other side, even if an early deflection does not extend the temporary capture phase sufficiently, a better-behaved temporary capture should be more suitable to prolong by thrusting throughout the capture phase. Thus, a two-step deflection strategy could also be proposed. Although an early deflection initiated relatively far from the Hill sphere crossing could increase launch costs, the actual deflection cost could be reduced considerably, so this option should be carefully investigated.

To explore this new approach, it is required to modify the numerical implementation of the previously adopted propagation scheme. As a reasonable time span, it is proposed to allow the deflection to begin up to 1000 days before the temporary capture. In this way, a backward propagation from the previously employed initial conditions is performed (segment 1) followed by a forward ballistic propagation of $d > 0$ days (segment 2), where the variable d stands for the delay of the thrust start date. Then, we propagate a trajectory arc with constant tangential thrust for ΔT days (segment 3) with a given (positive or negative) ΔV. Then, the thrust is stopped and the trajectory is propagated first until entering the Hill sphere (segment 4), and then until leaving the Hill sphere (segment 5).

Since we are interested in finding combinations of d, ΔT, and ΔV that yield well-behaved temporary captures, we decided to look for capture phases where the test particles remain for as long as possible, not just captured but strictly inside the Hill sphere, as is the behavior of 2006 RH_{120}. For that purpose, we performed grid searches in the parameters d, ΔT, and ΔV for the nine test cases listed in the previous section and limited to values $\Delta V \in \pm[0.5, 15]$ m/s. This would lead to relatively low-thrust levels, substantially smaller than 1 N, even assuming that the test particles have the same mass as 2006 RH_{120}. The results of these three-dimensional grid searches are remarkably positive in terms of extension of the capture phase; as for every single test particle, with the only exception of TP 9,[‡‡] we could extend their temporary capture for several years with thrust levels considerably below 1 N (in some cases, even as low as 30 mN).

After filtering the results to retain only trajectories spending over five years inside the Hill sphere, we can employ two-dimensional scatter plots to look for favorable combinations of d and ΔT, as in Fig. 16.

Observing analogous plots for test particles TP 1 to TP 8, we find that their orbits can indeed be modified to yield better-behaved long-lasting temporary captures. However, some of these trajectories come at the price of a reduced robustness of the extended capture phase: for instance, for TP 1, TP 2, and TP 7, there are only a few isolated trajectories (corresponding to different combinations of d and ΔT) that yield long-lifetime temporary captures. This means that, even though these improved captures exist, they may not be robust to small variations in the thrust parameters. For TP 4, TP 5, and TP 8, apart from isolated points, we also find traces that suggest some kind of order or pattern. Finally, for TP 3 and TP 6, we find clear patterns and isles of trajectories yielding long-lifetime temporary captures, which evidences these trajectories are robust to variations in the thrust parameters.

All these extended temporary captures were achieved with ΔV values smaller than ± 15 m/s. For TP 8, which already has an unmodified temporary capture of 500 days, a ΔV of just $+2$ m/s is enough to extend its capture lifetime. For test particles showing robust behavior, such as TP 3 or TP 6, a $|\Delta V|$ ranging from 5 to 10 m/s shows enough to attain the extended capture and, for those test particles with sparse combinations of d and ΔT that yield the desired temporary capture, values of $|\Delta V|$ beyond 10 m/s are required, which suggests that maybe higher ΔV values in the grid search could have provided more robust extended temporary captures.

Although in Fig. 16 we have filtered the grid search results to show only those spending over five years in the Hill sphere, there are actually some modified trajectories that spend several decades inside the Earth Hill sphere. For example, Fig. 17 shows modified trajectories of TP 3, corresponding to $\Delta V = 9$ m/s, which remains inside the Hill sphere (represented as a gray circle) for up to 36 years, with a required thrust of barely 40 mN.

Table 11 Best low-thrust extended capture (lowest-thrust criteria) for the nine test particles

	Extended temporary capture greater than 2 years		Extended temporary capture greater than 5 years	
Test particle	ΔV, m/s	Thrust, N	ΔV, m/s	Thrust, N
TP 1	−90.1	−3.30	−93.8	−5.17
TP 2	−69.0	−1.52	−64.9	−1.78
TP 3	−124.3	−5.66	−126.3	−5.98
TP 4	−137.2	−8.82	−140.5	−8.88
TP 5	−91.5	−1.73	−136.5	−3.06
TP 6	−77.6	−2.17	−72.5	−2.58
TP 7	−15.8	−0.70	−16.3	−0.80
TP 8	−67.0	−1.13	−71.0	−1.18
TP 9	Extension of the temporary capture is always below 2 years			

[‡‡]Remember, from the previous section, that TP 9 was also the only test particle for which the temporary capture could not be substantially increased: not even with an impulsive ΔV of reasonable magnitude.

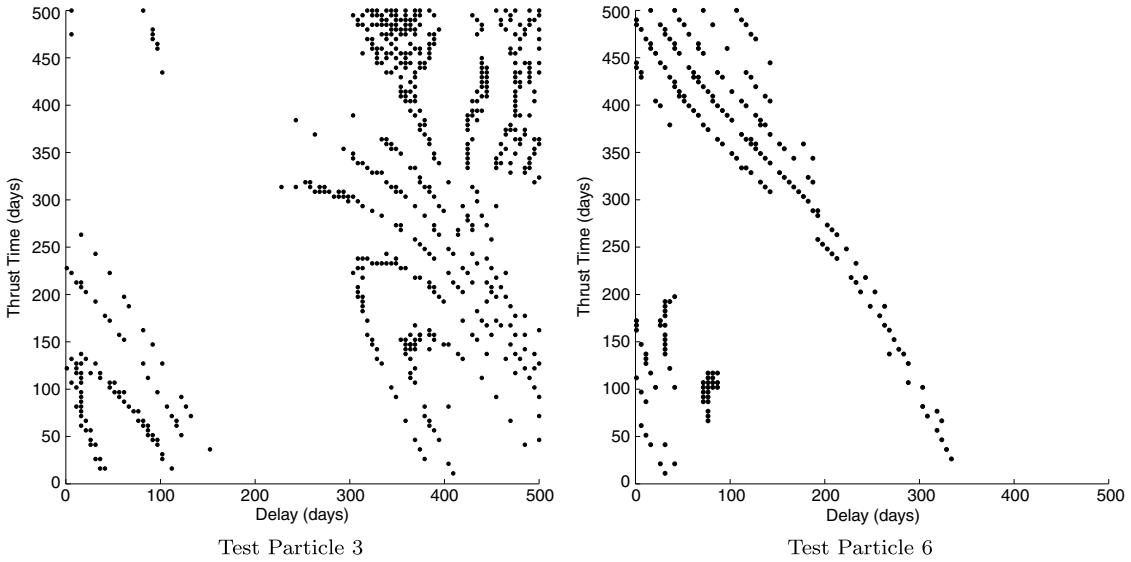

Fig. 16 Results of grid searches for TP 3 and TP 6.

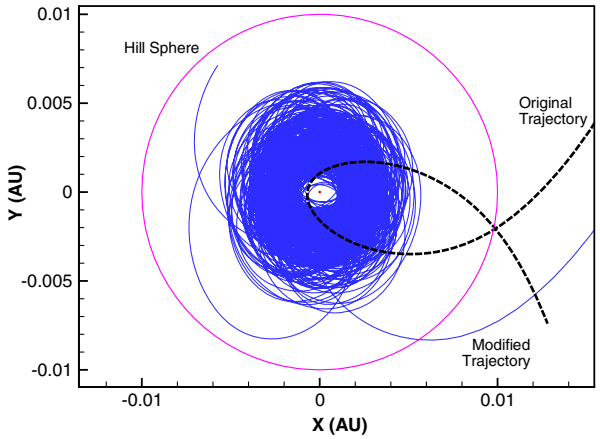

Fig. 17 Extended temporary capture of TP 3 lasting 13,202 days in the Hill sphere.

X. Conclusions

In this paper, a case study on extending the temporary capture phase of asteroid 2006 RH_{120}, which to date is the single known member of the population of temporarily captured objects of Earth, has been exposed. The study is also extended to nine other temporarily captured virtual asteroids.

According to the current simulations, it is concluded that, for temporarily captured asteroids, the study shows it is possible to prolong the duration of their capture phase with a slow deflection of their trajectory once the capture has begun, and by requiring low to moderate values of ΔV and low thrust.

More particularly, it has been estimated that deflecting asteroid 2006 RH_{120} during its past temporary capture during 2006–2007, with 0.274 N for about 172 days and a ΔV of 31.2 m/s, would have prolonged the duration of the capture for over five additional years.

Repeating the simulations for the considered virtual asteroids yields consistent results in terms of ΔV, although 2006 RH_{120} proves to be more favorable or better behaved than some of the other asteroids studied. Apparently, this is due to the nature of its temporary capture phase, which takes place completely inside the Hill sphere for most of its extent and completes several revolutions around the Earth; whereas other asteroids have shorter captures, taking place further from Earth and revolving slightly more than once around the Earth. Thus, some capture phases are more easily prolonged with a lower ΔV, depending on what their temporary capture is like.

In this regard, the possibility of deflecting the asteroids early before they begin their temporary capture has also been studied in order to modify or improve the nature of the capture phase, and thus turn it into a better-behaved or longer-lifetime capture. The current simulations show that, for most temporarily captured objects, with this strategy, it could be possible to extend their capture phases for several years, with ΔV values smaller than 15 m/s and a thrust intensity smaller than 1 N, assuming the same mass and size as 2006 RH_{120}.

Hence, assuming the current test particles are representative of the population of temporarily captured asteroids, these results suggest the following:

1) It should be possible for many temporarily captured objects to considerably extend the duration of their temporary capture phase with reasonably low ΔV values and low to moderate thrust levels by slowly deflecting their trajectory during the temporary capture.

2) It should be possible for most temporarily captured objects to considerably extend the duration of their temporary capture phase with low ΔV values and low-thrust levels by slowly deflecting their trajectory before the beginning of their temporary capture.

Finally, it is important to mention that, even though there are clear advantages of having an asteroid accessible in the vicinity of the Earth for future exploration missions (observation, communication, and operationalwise), the specific ΔV cost of reaching these orbits from Earth has not been addressed. Future studies shall look more in detail into the viability and cost of rendezvous transfer orbits to these temporarily captured asteroids.

Acknowledgments

The authors wish to acknowledge the Spanish Ministry of Economy and Competitiveness for their support through the research project “Dynamical Analysis, Advanced Orbital Propagation and Simulation of Complex Space Systems” (ESP2013-41634-P). Hodei Urrutxua acknowledges the Universidad Politécnica de Madrid for supporting his research through his Ph.D. program. Daniel J. Scheeres acknowledges support at the University of Colorado Boulder from NASA grant NNX14AB08G. The research leading to these results has received funding from the European Union Seventh Framework Programme (FP7/2007-2013) under grant agreement no. 317185 (Stardust). The authors also wish to thank Mikael Granvik, William F. Bottke, and Robert Jedicke for their careful reading of the manuscript, constructive feedback, and for facilitating the initial conditions for the temporarily captured test particles.

References

[1] Baoyin, H., Chen, Y., and Li, J., "Capturing Near Earth Objects," *Research in Astronomy and Astrophysics*, Vol. 10, No. 6, Aug. 2010, pp. 587–598. doi:10.1088/1674-4527/10/6/008

[2] Hasnain, Z., Lamb, C. A., and Ross, S. D., "Capturing Near-Earth Asteroids Around Earth," *Acta Astronautica*, Vol. 81, No. 2, 2012, pp. 523–531. doi:10.1016/j.actaastro.2012.07.029

[3] Sanchez, J. P., Yárnoz, D. G., Alessi, E. M., and McInnes, C. R., "Gravitational Capture Opportunities for Asteroid Retrieval Missions," *Proceedings of the 63rd International Astronautical Conference*, International Astronautical Federation IAC-12.C1.5.13x14763, Naples, Italy, 2012.

[4] Yárnoz, D. G., Sanchez, J. P., and McInnes, C. R., "Easily Retrievable Objects Among the NEO Population," *Celestial Mechanics and Dynamical Astronomy*, Vol. 116, No. 4, Aug. 2013, pp. 367–388. doi:10.1007/s10569-013-9495-6

[5] Bombardelli, C., Urrutxua, H., and Peláez, J., "Earth Delivery of a Small NEO with an Ion Beam Shepherd," *Advances in the Astronautical Sciences*, Vol. 143, Univelt, San Diego, CA, 2012, pp. 371–378.

[6] Brophy, J., Culick, F., Friedman, L., Allen, C., Baughman, D., Bellerose, J., Betts, B., Brown, M., Busch, M., Casani, J., Coradini, M., Dankanich, J., Dimotakis, P., Elvis, M., Garrick-Bethel, I., Gershman, B., Jones, T., Landau, D., Lewicki, C., Lewis, J., Llanos, P., Lupisella, M., Mazanek, D., Mehrotra, P., Nuth, J., Parkin, K., Schweickart, R., Singh, G., Strange, N., Tantardini, M., Wilcox, B., Williams, C., Williams, W., and Yeomans, D., "Asteroid Retrieval Feasibility Study," Keck Inst. for Space Studies, California Inst. of Technology, Jet Propulsion Lab., Pasadena, CA, April 2012.

[7] Granvik, M., Vaubaillon, J., and Jedicke, R., "The Population of Natural Earth Satellites," *Icarus*, Vol. 218, No. 1, 2012, pp. 262–277. doi:10.1016/j.icarus.2011.12.003

[8] Granvik, M., Jedicke, R., Bolin, B., Chyba, M., Patterson, G., and Picot, G., "Earth's Temporarily-Captured Natural Satellites—The First Step Towards Utilization of Asteroid Resources," *Asteroids: Prospective Energy and Material Resources*, Springer, Berlin, 2013, pp. 151–167, Chap. 6. doi:10.1007/978-3-642-39244-3_6

[9] Benner, L. A. M., "6R10DB9 Planning" California Inst. of Technology, Jet Propulsion Lab. /NASA Asteroid Radar Research, Pasadena, CA, June 2007, http://echo.jpl.nasa.gov/asteroids/6R10DB9/6R10DB9_planning.html.

[10] Standish, E. M., and Williams, J. G., "Orbital Ephemeris of the Sun, Moon and Planets," *Explanatory Supplement to the Astronomical Almanac*, Revised ed., Univ. Science Books, Sausalit, CA, Aug. 2005, Chap. 8.

[11] Jacobson, R. A., and Powers, W. F., "Optimal Low Thrust Escape Viewed as a Resonance Phenomenon," Univ. of Michigan TR-02677-T-2, Ann Arbor, MI, May 1970.

[12] Jolliffe, I. T., *Principal Component Analysis*," Springer Series in Statistics, 2nd ed., Springer, New York, 2002, pp. 10–26.

[13] MacQueen, J. B., "Some Methods for Classification and Analysis of Multivariate Observations," *Proceedings of the 5th Berkeley Symposium on Mathematical Statistics and Probability*, Vol. 1, Univ. of California Press, Oakland, CA, 1967, pp. 281–297.